Original Article

Mitochondrial reactive oxygen species accelerate gastric cancer cell invasion

Masato Tamura,[1] Hirofumi Matsui,[1,*] Tsutomu Tomita,[2] Hisato Sadakata,[2] Hiroko P. Indo,[3] Hideyuki J. Majima,[3] Tsuyoshi Kaneko[1] and Ichinosuke Hyodo[1]

[1]Faculty of Medicine and [2]Graduate School of Pure and Applied Sciences, University of Tsukuba, 1-1-1 Ten-noudai, Tsukuba, Ibaraki 305-8573, Japan
[3]Medical and Dental Sciences, Kagoshima University, 8-35-1 Sakuragawa, Kagoshima, Japan

(Received 9 April, 2013; Accepted 30 April, 2013; Published online 9 November, 2013)

Tumor invasion is the most important factor to decide patient's prognosis. The relation between reactive oxygen species and tumor invasion is mainly reported that nicotinamide adenine dinucleotide phosphate oxidase in the cell membrane is a reactive oxygen species producer for formulating an invadopodia. On the other hand, mitochondrion was known as one of the most important reactive oxygen species-producer in the cell via an energy transfer system. However, the relation between mitochondrial reactive oxygen species and the tumor invasion was not well clarified. In this study, we evaluated the relation between mitochondrial reactive oxygen species and tumor invasion using a normal gastric mucosal cell-line (RGM-1) and a cancerous mutant RGM-1 cell-line (RGK-1). Manganese superoxide dismutase-expressing RGK-1 cell-lines were used for a scavenging mitochondrial reactive oxygen species. The cells have been evaluated their movement ability as follows; cellular ruffling frequencies, wound healing assay to evaluate horizontal cellular migration, and invasion assay using matrigel to analyze vertical cellular migration. All cellular movement abilities were inhibited by scavenging mitochondrial reactive oxygen species with manganese superoxide dismutase. Therefore mitochondrial reactive oxygen species was one of factors enhancing the tumor invasion in gastric cancer.

Key Words: **reactive oxygen species, mitochondria, tumor invasion, electron paramagnetic resonance, manganese superoxide dismutase**

Cancer cellular reactive oxygen species (ROS) play an important role in their proliferation, invasion and metastasis.[1,2] The ROS regulates tumor invasion through actin remodeling proteins and focal adhesion proteins.[3,4] Tumor invasion ability is the most important factor to decide patient's prognosis. Tumors without invading abilities are usually diagnosed as benign lesions, and treatments decreasing these abilities possibly improve the prognosis. NADPH oxidase (NOX) was mainly reported to generate ROS involving tumor invasion. NOX is an enzyme located in cellular membrane to produce superoxide anion ($O_2^{\bullet}$) which accelerates invadopodia formation.[5–8]

Mitochondrion is a main source of ROS, because it used to show complex I dysfunction to generate $O_2^{\bullet}$ in cancer cells. This dysfunction is induced by cancerous gene mutation.[9] Mitochondrial ROS derived cancer cellular progression and metastasis.[10–12] However, the relation between mitochondrial ROS and tumor invasion is not well investigated.

Manganese superoxide dismutase (MnSOD) is particularly localized at mitochondria to scavenge their $O_2^{\bullet}$.[13,14] Overexpression of MnSOD after its gene transfection suppressed tumor proliferation and metastasis.[11] Mitochondrial ROS is thus likely to important for organizing tumor properties.

Recently we established two cell lines; a rat normal gastric mucosa cell-lines (RGM-1) and a cancerous RGM-1 cell-lines (RGK-1).[15] These cell lines are useful to compare cellular properties between normal cells and cancerous cells. In addition, we also established MnSOD-expressing cell lines, because these cell-lines used to be regarded as good experimental materials to clarify whether intracellular ROS were derived from mitochondria or not.[12,16–21] Using them, we have reported the roles of mitochondrial ROS to involve gastric epithelial cellular injuries after treatments with NSAIDs, bisphosphonate and exposure to acidic environments.[22,23]

In this study, we elucidated whether mitochondrial ROS involved tumor cellular invasion or not. For this aim, we investigated living cellular ROS spectra of electron paramagnetic resonance (EPR) using RGM-1, RGK-1 and MnSOD-overexpressing stable clone RGK-1 cell lines (RGK-1 MnSOD). We also evaluated cellular ruffling frequencies, wound healing assay and invasion assay as described in "Materials and Methods".

Materials and Methods

Materials. Aminophenyl Fluorescein (APF) (SEKISUI MEDICAL CO., LTD., Tokyo, Japan), and 2-[5,5-Dimethyl-2-oxo-2λ5-(1,3,2)dioxaphosphinan-2-yl]-2-methyl-3,4-dihydro-2H-pyrrole 1-oxide (CYPMPO) (Radical Research Inc., Tokyo, Japan) were purchased. Can get signal (PVDF blocking reagent, Solution 1, Solution 2) and WB Stripping Solution Strong (Nacalai tesque Inc., Kyoto, Japan) were used for western blotting analysis.

Cell culture. RGM-1 and RGK-1 were cultured in DMEM/F12 (Life Technologies Co., CA) and Dulbecco's modified EAGLE'S medium nutrient mixture F-12 HAM (Life Technologies Co.), respectively. These culture mediums contains 10% inactivated FBS and 1% penicillin/streptomycin. Culture medium for RGK-1 MnSOD also contained antibiotic G418 sulfate for being stable MnSOD expression. Gene vector transfected RGK-1 cell line was used as the control for a gene transfect. The different number in RGK-1 MnSOD means different clone like RGM-1 MnSOD-overexpression cell lines.[16] Each cells showed differ MnSOD-expression. All cells were cultured in 5% CO_2 cell culture incubator at 37°C.

ROS measurement by EPR. EPR measurement was performed according to previous report.[24] Briefly, cells were cultured on cover slide glasses ($49 \times 5 \times 0.2$ mm). Cells were immersed in culture medium with 5 mM respiratory substrates (succinate, glutamate, and malate), 5 mM nicotinamide adenine

*To whom correspondence should be addressed.
E-mail: hmatsui@md.tsukuba.ac.jp

doi: 10.3164/jcbn.13-36
©2014 JCBN

dinucleotide (NADH) and 10 mM CYPMPO. Immersed-slide glasses were put on the tissue glass, thereafter the couple of glasses were measured by EPR apparatus.

Standard signals of H_2O_2 by Fenton reaction and $O_2^{\bullet}$ by xanthine/xanthine oxidase reaction were studied according to the report.[25] Briefly, same volume of 10 mM CYPMPO, 0.1 mM H_2O_2, 50 mM PBS (pH 7.4) and 3 mM $FeSO_4$ were mixed for Fenton reaction, and the mixture was analyzed by EPR. For xanthine/xanthine oxidase reaction, 50 mM CYPMPO, 2 mM hypoxanthine, 0.4 U/mL xanthine oxidase and 50 mM PBS (pH 7.4) were mixed, and the mixture was used as $O_2^{\bullet}$ standard.

All EPR spectra were recorded by using a JEOL-TE X-band spectrometer (JEOL Ltd., Tokyo, Japan). All EPR spectra were obtained under the following conditions: 10 mW incident microwave power, 9.42 GHz frequency, 0.1 mT field modulation amplitude, and 15 mT scan range. The hyperfine splitting constants (hfsc) and spectral computer simulation were analyzed using a Win-Rad Radical Analyzer System (Radical Research Inc.). All EPR spectra were representative of at least 3 independent experiments.

Measurements of oxidative stress by APF. Free radicals (hydroxyl radical and peroxynitrite) were detected by APF as follows; APF was diluted with PBS and it exposed to the cells at the concentration of 1 μM for 30 min. After incubation, cells were washed using a cold PBS twice. The intensities of APF-fluorescent were measured by Varioskan (Thermo Fisher Scientific K.K., Kanagawa, Japan) at Ex. 490 nm and Em. 515 nm.

Western blotting analysis. Western blotting analysis was studied according to previous reports.[26] Briefly, the protein from cell-lysate was obtained according to RIPA buffer manufacture's protocol. The amount of total protein in sample solution was determined using Protein Quantification kit - Rapid (Dojindo Molecular Technologies, Inc., Kumamoto, Japan). The electrophoresis and the blotting procedure were studied as follows; 15 μl (10 μg) protein samples were applied in the well of NuPAGEgel (Life technologies). After the samples were applied in the lane, it was electrophoresed under 200 V for 30 min on ice. And then, proteins were blotted to PVDF membrane under 30 V for 10 min.

The definition of protein using sandwich immune assay were performed according to manufacture protocol of SNAP i.d. (Millipore Co., MA). Rabbit polyclonal MnSOD antibody (Enzo Life Sciences, Inc., NY) and β-actin rabbit antibody (Cell Signaling Technology, K.K., Tokyo, Japan) were used as first anti-body, and anti-rabbit IgG HRP-linked antibody (Cell Signaling Technology) was used as second anti-body. After Luminata forte western HRP substrate (Millipore) added, luminescence was detected by LAS4000 (GE Health care Japan Co., Ltd., Tokyo, Japan).

Evaluation of cell membrane ruffling. Cell membrane ruffling was determined with a method of Borm *et al*.[27] Briefly, the movie was created by 75 pictures (1 pictures/min). The movie was changed a black-and-white image (8 bit, tone; 256, Black; less than tone 80, white; more than tone 80), and the region of interest (ROI: 5,000 pixels/each movies) was set around the cells. Ruffling frequencies were calculated based on the sum of dark area of the movies using Image J software ver. 1.43 (National Institute of Health, MA).

Wound healing assay. Wound healing assay was studied according to previous report.[28] Briefly, the free-cell area was created using yellow-chip on the confluent cell. After incubated for 0, 6, 12 and 24 h, The free-cell area (μm^2) was measured on the microscopic picture by the analysis software (ZEN software, Carl Zeiss Co., Ltd., Jena, Germany).

Tumor invasion assay. Matrigel was created in the well of 96-well plate. 50 μl Matrigel solutions were poured to the well at 4°C, and then the plate was incubated at 37°C for 30 min. After polymerization of matrigel, the cells (RGM-1, RGK-1, RGK-1 MnSOD2, RGK-1 MnSOD3 and RGK-1 MnSOD9; 500 cells/well) were dispersed on matrigel and it was incubated for 24 h. After cells were attached on the matrigel, the invasion assay was started (this time was 0 h in Fig. 6). The invaded-length was taken a pictured using the z-stack function of confocal microscopy after 0, 24 and 48 h. The pictures were obtained 6.02 μm/slice through z-axis movement. The measurement of invaded-length was calculated based on 3D matrigel pictures, those were created by 2D pictures. This experiment was studied twice independently.

Statistical analysis. Statistical analysis was calculated on the Origin software. Significant static value (*p* value) was calculated using ANOVA followed by Scheffe's F-test.

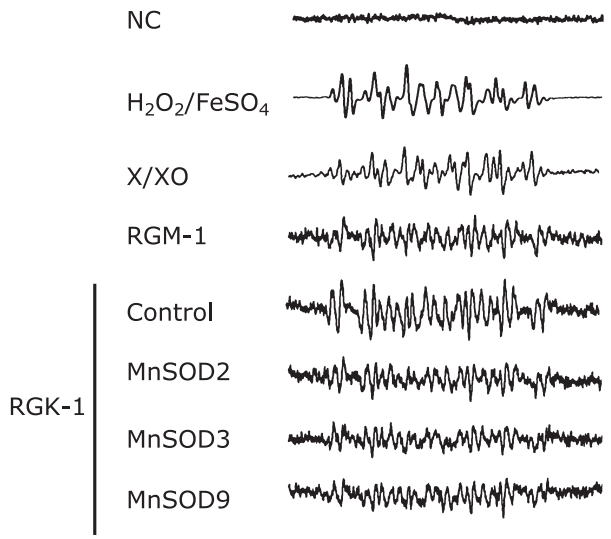

Fig. 1. Cellular ROS concentration in living cells by EPR. CYPMPO was used as a spin trapping reagent.

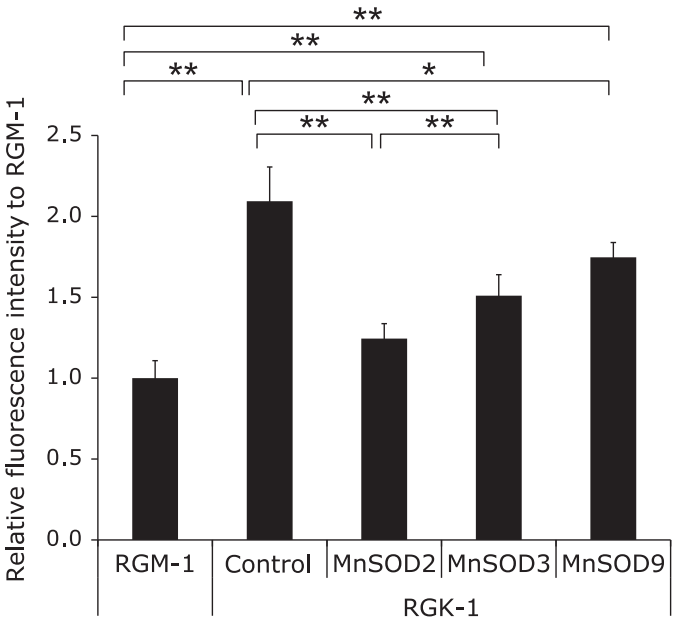

Fig. 2. Cellular ROS concentration of RGM-1, RGK-1 control, RGK-1 MnSOD2, RGK-1 MnSOD3, and RGK-1 MnSOD9. The cellular ROS concentration was detected by APF. The MnSOD expression decreased the cellular ROS concentration significantly. The data are expressed as mean ± SD (n = 6). *p<0.05, **p<0.01.

©2014 JCBN

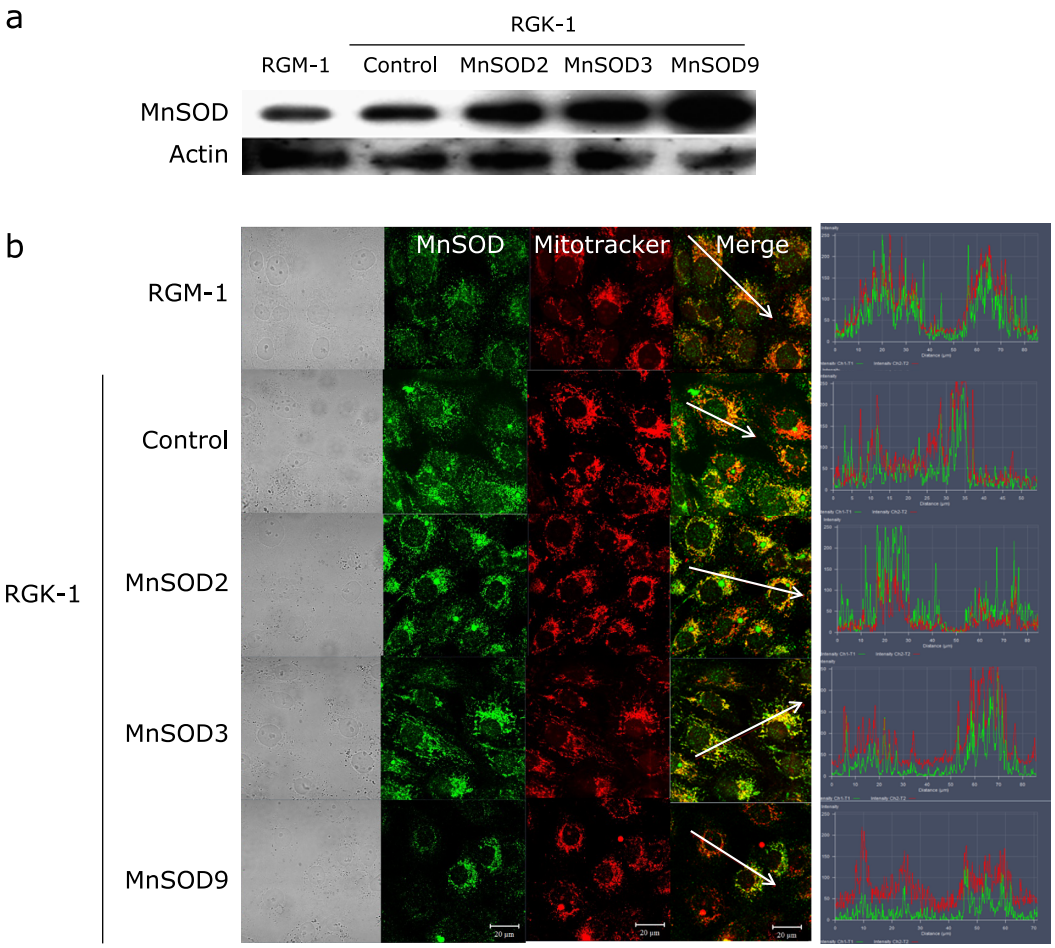

Fig. 3. Determination of the amount of MnSOD by Western blotting analysis and the colocarization of MnSOD and mitochondria. (a) Western blotting analysis of MnSOD. (b) MnSOD was immunostained with FITC labeled second antibody and mitochondria was stained with Mitotracker Red. The change of their fluorescent intensity showed almost same tendency.

Results

Cellular ROS concentration in normal cells and cancerous mutant cells. Generally, cancerous cells used to show higher ROS concentration than that of normal cells. We have evaluated the intracellular ROS concentration of two cell-lines. One is a normal RGM-1, and another is a RGK-1.[15] The intracellular ROS concentration was determined by EPR measurement with a spin trap reagent CYPMPO. Standard spectra of H_2O_2 by Fenton reaction and $O_2\cdot$ by xanthine/xanthine oxidase reaction showed different EPR spectra from that of living cells (Fig. 1). RGK-1 spectrum of EPR was stronger than that of RGM-1 (Fig. 1). Additionally, we have measured cellular ROS with a fluorescent dye APF, of which intensity can be a representative of the amounts of hydroxyl radicals and peroxynitrite.[29] The intensity of RGK-1 was about twice higher than that of RGM-1 (Fig. 2).

MnSOD-expression and subcellular location in RGK-1 MnSOD. The amount of MnSOD expressed in each cell-line was determined by Western blotting analysis and digitalized calculations of MnSOD expression with immunohistochemically stained specimens, respectively (Fig. 3). The transfected MnSOD vector has the mitochondrial targeting sequences, the expressing-MnSOD can thereby scavenge mitochondrial ROS particularly.[16] After the gene vector transfection, the amount of MnSOD in RGK-MnSOD was larger than that of non-gene transfected RGK-1 (Fig. 3a), and these MnSOD was colocalized with

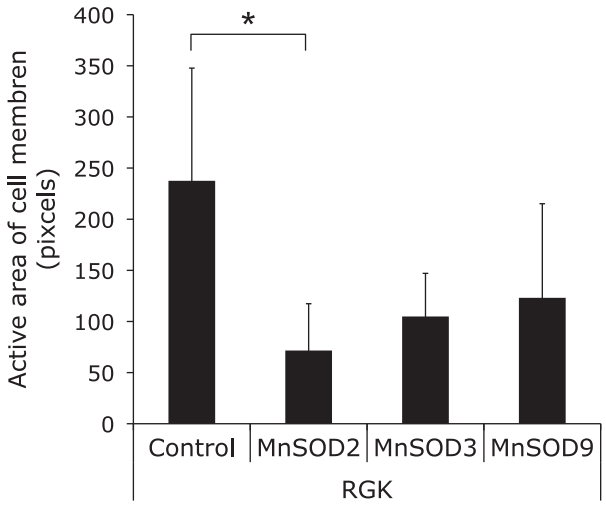

Fig. 4. Determination of cellular ruffling activity. These data shows the average ruffling area in 5000 pixels of pictures. MnSOD reduced the cellular ruffling activity. The data are expressed as mean ± SD. (n = 6), *p<0.05.

doi: 10.3164/jcbn.13-36
©2014 JCBN

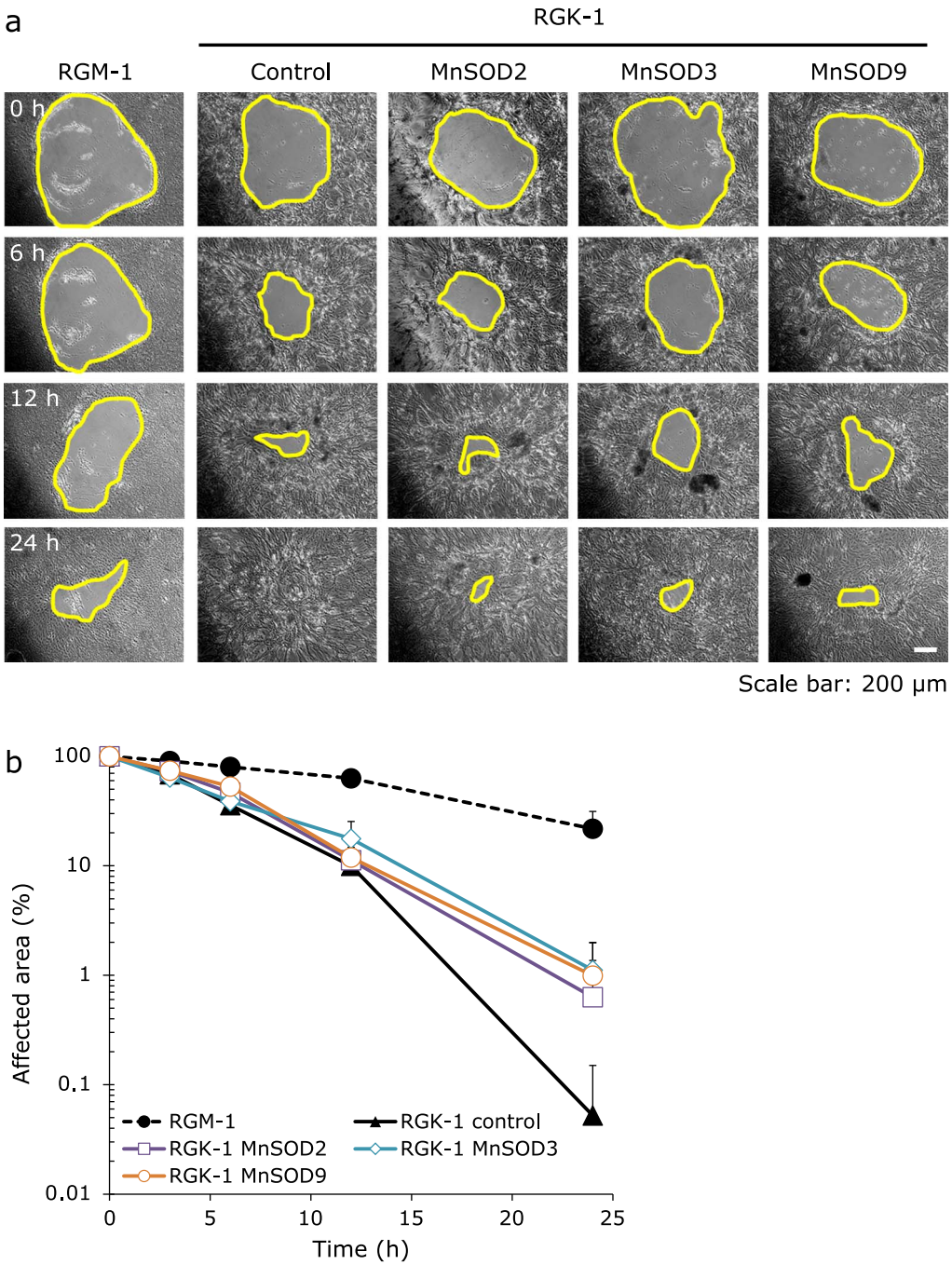

Fig. 5. Wound healing assay. (a) The pictures of free-cell area. The free-cell area was surrounded with yellow line. (b) The percentage of affected area compared as the pore size incubated after 0 h. These results indicated that the migration is enhanced by tumorigenesis and it was decreased reducing cellular ROS-concentration by MnSOD. The data are expressed as mean ± SD (n = 6).

mitochondria (Fig. 3b). Fig. 1 and Fig. 2 show intracellular ROS concentration of RGK-1 MnSOD. The EPR spectra of these RGK-1 MnSOD cells were weaker signals than that of RGK-1 control. Together, these results indicated that mitochondrial ROS were scavenged by MnSOD. The ROS concentration in RGK-1 was significantly higher than in normal cells, and MnSOD overexpression significantly decreased this cancer specific higher ROS concentration.

Scavenging mitochondrial ROS by MnSOD decreased cellular ruffling frequencies. Supporting information Supplemental Table 1 shows the analytical results of cellular movement assays in this research. The cellular ruffling activity is one of essential movement relating cellular migration. The expression of MnSOD decreased cellular ruffling significantly (Fig. 4). These data of ruffling frequencies showed same tendency of the intracellular ROS concentration.

Scavenging mitochondrial ROS by MnSOD suppressed horizontal cellular migration and cell invasion to matrigel. The relation between horizontal cellular migration and mitochondrial ROS was evaluated. The wound healing assay was studied as the evaluation of horizontal cellular migration. The results of wound healing assay might be affected by the cell growth. There-

*See online. https://www.jstage.jst.co.jp/article/jcbn/54/1/54_13-36/_article/supplement

©2014 JCBN

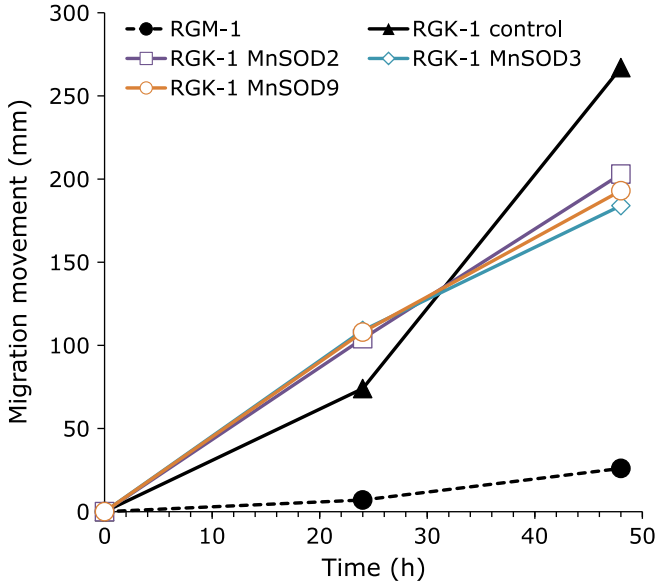

Fig. 6. Invasion assay using matrigel. The cells (500 cells/100 μl) were harvested on matrigel and incubated overnight. After cells were attached, it was took pictures using the z-stack function of confocal microscopy (6.02 μm/slices) for 0, 24 and 48 h. 3D structure picture was created based on obtained-2D-pictures on the axio-vision software. The invaded-length was measured on the 3D picture. This assay was experimented twice, and the tendency of invasion was same.

fore we have evaluated at first the cell growth speed (Supplemental Fig. 1). There were no significant differences in each RGK-1 cell lines. The results of wound healing assays indicated that the fastest cell-line of horizontal cellular migration ability was RGK-1, RGK-1 MnSOD was the second one and RGM-1 was the latest one (Fig. 5). These results indicated that mitochondrial ROS played an important role in cellular migration.

Scavenging mitochondrial ROS by MnSOD inhibited the cellular invasion to matrigel. To elucidate the relation between cellular invading abilities and ROS, we measured length of each cellular invasion into matrigel layer, an artificial model of extracellular matrix.[30,31] The length of vertical cellular migration from the top of matrigel to the deepest cells with a confocal microscopy was measured. These results showed the same tendency of horizontal cellular migration: the RGK-1 showed the highest performance of invasion ability, RGK-1 MnSOD showed the second one and RGM-1 showed the lowest (Fig. 6).

Discussion

The intracellular ROS concentration in RGK-1 was about twice higher than that in RGM-1 according to the results of EPR measurement using living cells. RGK-MnSOD significantly decreased intracellular ROS concentration. We thus concluded that cancerous mutation involved mitochondrial ROS production. The eliminated-mitochondrial ROS should be superoxide anion because MnSOD reduced the intensity of ESR spectra in RGK-1.

The tumor cellular invasion has suppressed by scavenging mitochondrial ROS. Cellular invasion needs alteration of cellular morphology including invadopodia to move. The data suggested the participation of Tropomyosin 1 and NOX-derived superoxide anion for forming invadopodia, which show an obvious amount in RGK-1 but few in RGM-1.[6,7,32–34] These factors should be impaired by expressed MnSOD. We confirmed the activation of cytoskeletal-associated protein due to clarify the mechanism of cellular movements through a mitochondrial ROS. However the amount of Rac1/cdc42 did not reduce by the expression of MnSOD (data not shown). The mitochondrial ROS might have a different mechanism for the tumor invasions from the NOX-ROS pathway. Cellular invasion also needs the ability of degrading collagens to create the road in extracellular matrix. Mitochondrial ROS controls matrix metalloproteinase signaling (MMP) by activating MMP gene expression or proenzymes.[35] MMP enhances tumor invasion ability by degrading collagens. MMP signals may play an important role for tumor invasion. We now under-investigate it.

Conclusions

We demonstrated for the first time that mitochondrial ROS involved cancer cellular invasion. The intensity of EPR spectra from RGK-1 cells was twice higher than that of RGM-1 cells, and this EPR signals was decreased by scavenging mitochondrial ROS. The cellular membrane ruffling, cellular migration and cell invasion were suppressed by scavenging mitochondrial ROS.

Acknowledgments

This work was partially supported by the Japan Society for the Promotion of Science (JSPS) and Grant-in-Aid for Scientific Research (KAKENHI) #24106503, #70272200. We are grateful to Japanese Meeting on Digestive Diseases and Free Radicals.

Conflict of Interest

No potential conflicts of interest were disclosed.

References

1 Nishikawa M. Reactive oxygen species in tumor metastasis. *Cancer Lett* 2008; **266**: 53–59.
2 Wu WS. The signaling mechanism of ROS in tumor progression. *Cancer Metastasis Rev* 2006; **25**: 695–705.
3 Schmitz AA, Govek EE, Böttner B, Van Aelst L. Rho GTPases: signaling, migration, and invasion. *Exp Cell Res* 2000; **261**: 1–12.
4 Raftopoulou M, Hall A. Cell migration: Rho GTPases lead the way. *Developmental Biology* 2004; **265**: 23–32.
5 Gianni D, Diaz B, Taulet N, Fowler B, Courtneidge SA, Bokoch GM. Novel p47(phox)-related organizers regulate localized NADPH oxidase 1 (Nox1) activity. *Sci Signal* 2009; **2**: ra54.
6 Montezano AC, Burger D, Ceravolo GS, Yusuf H, Montero M, Touyz RM. Novel Nox homologues in the vasculature: focusing on Nox4 and Nox5. *Clin Sci (Lond)* 2011; **120**: 131–141.
7 Weaver AM. Regulation of cancer invasion by reactive oxygen species and Tks family scaffold proteins. *Sci Signal* 2009; **2**: pe56.
8 Kumar B, Koul S, Khandrika L, Meacham RB, Koul HK. Oxidative stress is inherent in prostate cancer cells and is required for aggressive phenotype. *Cancer Res* 2008; **68**: 1777–1785.
9 Taddei ML, Giannoni E, Raugei G, *et al*. Mitochondrial Oxidative Stress due to Complex I Dysfunction Promotes Fibroblast Activation and Melanoma Cell Invasiveness. *J Signal Transduct* 2012; **2012**: 684592.
10 Zhong W, Oberley LW, Oberley TD, St Clair DK. Suppression of the malignant phenotype of human glioma cells by overexpression of manganese superoxide dismutase. *Oncogene* 1997; **14**: 481–490.
11 Sotgia F, Martinez-Outschoorn UE, Lisanti MP. Mitochondrial oxidative stress drives tumor progression and metastasis: should we use antioxidants as a key component of cancer treatment and prevention? *BMC Med* 2011; **9**: 62.
12 Indo HP, Davidson M, Yen HC, *et al*. Evidence of ROS generation by mitochondria in cells with impaired electron transport chain and mitochondrial DNA damage. *Mitochondrion* 2007; **7**: 106–118.
13 Okado-Matsumoto A, Fridovich I. Subcellular distribution of superoxide

*See online. https://www.jstage.jst.co.jp/article/jcbn/54/1/54_13-36/_article/supplement

doi: 10.3164/jcbn.13-36
©2014 JCBN

dismutases (SOD) in rat liver: Cu,Zn-SOD in mitochondria. *J Biol Chem* 2001; **276**: 38388–38393.
14 Zhang HJ, Yan T, Oberley TD, Oberley LW. Comparison of effects of two polymorphic variants of manganese superoxide dismutase on human breast MCF-7 cancer cell phenotype. *Cancer Res* 1999; **59**: 6276–6283.
15 Shimokawa O, Matsui H, Nagano Y, *et al*. Neoplastic transformation and induction of H+, K+ -adenosine triphosphatase by N-methyl-N'-nitro-N-nitrosoguanidine in the gastric epithelial RGM-1 cell line. *In Vitro Cell Dev Biol Anim* 2008; **44**: 26–30.
16 Motoori S, Majima HJ, Ebara M, *et al*. Overexpression of mitochondrial manganese superoxide dismutase protects against radiation-induced cell death in the human hepatocellular carcinoma cell line HLE. *Cancer Res* 2001; **61**: 5382–5388.
17 Indo HP, Inanami O, Koumura T, *et al*. Roles of mitochondria-generated reactive oxygen species on X-ray-induced apoptosis in a human hepatocellular carcinoma cell line, HLE. *Free Radic Res* 2012; **46**: 1029–1043.
18 Majima HJ, Indo HP, Suenaga S, *et al*. Mitochondria as Source of Free Radicals. *Free Radical Biology* 2011; **29**: 12–22.
19 Majima HJ, Oberley TD, Furukawa K, *et al*. Prevention of mitochondrial injury by manganese superoxide dismutase reveals a primary mechanism for alkaline-induced cell death. *J Biol Chem* 1998; **273**: 8217–8224.
20 Majima HJ, Indo HP, Suenaga S, Matsui H, Yen HC, Ozawa T. Mitochondria as possible pharmaceutical targets for the effects of vitamin E and its homologues in oxidative stress-related diseases. *Current Pharm Des* 2011; **17**: 2190–2195.
21 Rai K, Matsui H, Kaneko T, *et al*. Lansoprazole inhibits mitochondrial superoxide production and cellular lipid peroxidation induced by indomethacin in RGM1 cells. *J Clin Biochem Nutr* 2011; **49**: 25–30.
22 Nagano Y, Matsui H, Tamura M, *et al*. NSAIDs and acidic environment induce gastric mucosal cellular mitochondrial dysfunction. *Digestion* 2012; **85**: 131–135.
23 Nagano Y, Matsui H, Shimokawa O, *et al*. Bisphosphonate-induced gastrointestinal mucosal injury is mediated by mitochondrial superoxide production and lipid peroxidation. *J Clin Biochem Nutr* 2012; **51**: 196–203.
24 Matsui H, Nagano Y, Shimokawa O, *et al*. Gastric acid induces mitochondrial superoxide production and lipid peroxidation in gastric epithelial cells. *J Gastroenterol* 2011; **46**: 1167–1176.
25 Mukohda M, Ueno S, Kamibayashi M, Okada M, Yamawaki H, Hara Y. Influences of organic solvents on CYPMPO-electron spin resonance spectra in *in vitro* radical generating systems. *J Vet Med Sci* 2010; **72**: 1547–1550.
26 Kuroda M, Yoshida N, Ichikawa H, *et al*. Lansoprazole, a proton pump inhibitor, reduces the severity of indomethacin-induced rat enteritis. *Int J Mol Med* 2006; **17**: 89–93.
27 Borm B, Requardt RP, Herzog V, Kirfel G. Membrane ruffles in cell migration: indicators of inefficient lamellipodia adhesion and compartments of actin filament reorganization. *Exp Cell Res* 2005; **302**: 83–95.
28 Yarrow JC, Perlman ZE, Westwood NJ, Mitchison TJ. A high-throughput cell migration assay using scratch wound healing, a comparison of image-based readout methods. *BMC Biotechnol* 2004; **4**: 21.
29 Setsukinai K, Urano Y, Kakinuma K, Majima HJ, Nagano T. Development of novel fluorescence probes that can reliably detect reactive oxygen species and distinguish specific species. *J Biol Chem* 2003; **278**: 3170–3175.
30 Albini A, Iwamoto Y, Kleinman HK, *et al*. A rapid *in vitro* assay for quantitating the invasive potential of tumor cells. *Cancer Res* 1987; **47**: 3239–3245.
31 Terranova VP, Hujanen ES, Loeb DM, Martin GR, Thornburg L, Glushko V. Use of a reconstituted basement membrane to measure cell invasiveness and select for highly invasive tumor cells. *Proc Natl Acad Sci U S A* 1986; **83**: 465–469.
32 Okada H, Naito Y, Takagi T, *et al*. Detection of *N*-(hexanoyl)lysine in the tropomyosin 1 protein in *N*-methyl-*N*'-nitro-*N*-nitrosoguanidine-induced rat gastric cancer cells. *J Clin Biochem Nutr* 2012; **50**: 47–52.
33 Gianni D, Taulet N, Zhang H, *et al*. A novel and specific NADPH oxidase-1 (Nox1) small-molecule inhibitor blocks the formation of functional invadopodia in human colon cancer cells. *ACS Chem Biol* 2010; **5**: 981–993.
34 Diaz B, Shani G, Pass I, Anderson D, Quintavalle M, Courtheidge SA. Tks5-dependent, nox-mediated generation of reactive oxygen species is necessary for invadopodia formation. *Sci Signal* 2009; **2**: ra53.
35 Touyz RM. Mitochondrial redox control of matrix metalloproteinase signaling in resistance arteries. *Arterioscler Thromb Vasc Biol* 2006; **26**: 685–688.

©2014 JCBN